# Design, synthesis and application of paramagnetic NMR ptobes for protein strucutre studies

Miao, Q.

# Chapter III

# A hydrophilic paramagnetic NMR probe for lanthanoid ions and 3d-block ions

# *Chapter III*


**Abstract**

A new DOTA based transition metal ion paramagnetic NMR probe (TraNP2) was designed and synthesized. TraNP2 can tightly chelate both lanthanoids and 3d-block metal ions. Its paramagnetic properties were studied after attachment to T4 Lysozyme mutant K147C/T151C. NMR spectra of the amide groups of T4Lys tagged with Yb(III)-TraNP2 showed two sets of PCS, suggesting presence of at least two conformers. Surprisingly, Co(II) loaded TraNP2 linked to the T4Lys mutant induces only very small PCS. The paramagnetic properties of Co(II)-TraNP2 complex were studied by measuring the effective magnetic moment ($\mu_{B,\ eff}$). The results showed that Co(II)-TraNP2 is indeed paramagnetic. The reason why the PCS are so small remains unclear.

**Introduction**

The use of small ligands able to bind paramagnetic metal ions that can be applied as probes in paramagnetic NMR is becoming an important strategy to study protein dynamics.[1–3] With different metal ions, various paramagnetic effects can be obtained. Lanthanoids are the common metal ions used for paramagnetic NMR, due to their similar chemical properties and variable paramagnetic effects.[4,5] 3d-Block metal ions can also be used to generate somewhat weaker paramagnetic effects. For example, cobalt (II) generates an anisotropic magnetic tensor from 2 to 10 x $10^{-32}$ $m^3$ with a weak PRE effect, which is suitable to study small proteins or localized effects in bigger systems.[6–9] Manganese (II) does not induce PCS but can produce a strong PRE effect, due to five unpaired electrons and a long electronic relaxation time.[7,10,11] The coordination requirements in terms of numbers and geometry differ considerably between these two groups of ions.

According to Werner's coordination theory,[12] two types of valence contribute to metal ion coordination, one related to the oxidation state of the ion and another related to its coordination numbers. Satisfying both valences leads to the lowest energy structure. Commonly, 3d-block ions have various oxidation states and require four to six coordination donors.[13] Their geometries, which are well explained by crystal field theory[14,15], are tetrahedral, square pyramidal and octahedral (Figure 1.4, Chapter I). Lanthanoid ions are stable in +3 oxidation state and need seven to nine coordination sites.[16] Different from 3d-block ions, the coordination geometries of Ln(III) are less studied.[17] Few reported paramagnetic NMR probes are able to coordinate both Ln(III) and 3d-block ions. Among these probes, multiple sets of PCS were detected or additional coordination from a protein side chain was required.[10,18] As described in chapter I, sections 3.3.4.1 and 3.3.4.2, probe **46** and probe **51** (Figure 1.10, Chapter I) are the only two that can chelate both group ions. Probe **46** needs additional coordination of a protein side chain, and Co(II) loaded probe **51** generated two sets of PCS. Also, the metal ion binding affinity was poor.

Here, we describe a probe that is able to bind to both 3d-block ions and lanthanoid ions. In Leiden, several successful Ln(III) based probes, such as CLaNP5[19] and CLaNP7[20], were designed and synthesized. However, these probes are not suitable for 3d-blok ions, like Co(II) and Mn (II). In chapter II, the design and synthesis of TraNP1 (transition metal NMR probe # 1) was described. It coordinates Co(II) and generates a single set of paramagnetic effects in a tagged protein, but it is not a good chelator for Ln(III). As part of that effort, we also designed an isomer of TraNP1 with different coordination arms (Figure 3.1). The effect of the branching of the carbons of two opposing arms is anticipated to reduce the number of conformers. Previously, branched side-arms having methyl-groups have been reported.[21,22] We introduced methylene hydroxyl groups to ensure a more hydrophilic probe, to avoid precipitation of the tagged

proteins. According to the NMR spectra, TraNP2 is a good ligand for both Co(II) and Yb(III). However, multiple PCS were observed for Yb(III)-TraNP2 attached protein, whereas small PCS were detected for a protein tagged with Co(II)-TraNP2.

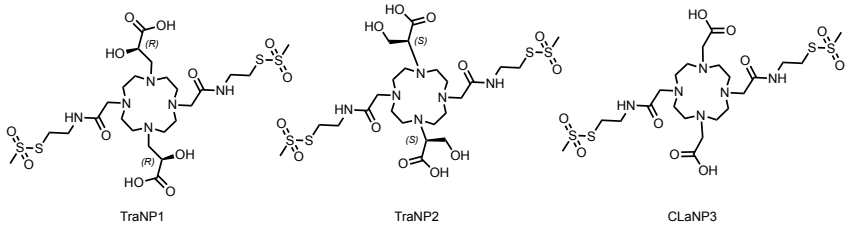


**Figure 3.1** Structure of TraNP1, TraNP2 and CLaNP3

**Results and Discussion**

**Design and synthesis of TraNP2.** The most used and well-studied cyclen based chelator is DOTA (chapter 1, Figure 1.8), which has high metal binding affinity to form thermodynamically stable complexes.[23,24] Instead of using acetate groups as coordination arms, a pair of methyl hydroxyl groups substituted analogous was used as coordination arms for TraNP2 with the aim to reduce the number of conformers (Figure 3.1). These two chiral groups were incorporated at the opposing nitrogens to ensure a $C_2$ symmetry. A frequently applied strategy to synthesize a $C_2$ symmetric cyclen derivative is via a selective protection and alkylation strategy. However, this strategy proved unsuccessful for the synthesis of TraNP2. The synthetic route of TraNP2 is shown in Scheme 3.1. Cyclen was first alkylated with two equiv. of **1**, readily obtained from the amino acid serine via its diazonium salt[25], in the presence of DIPEA. LC-MS, showed that after 48 h at rt, no starting compound was detected and that the main product was the desired di-alkylated compound (only small amounts of mono and tri-alkylated products were observed). The obtained crude product was used to react with excess S-(2-(2-bromoacetamido)ethyl)

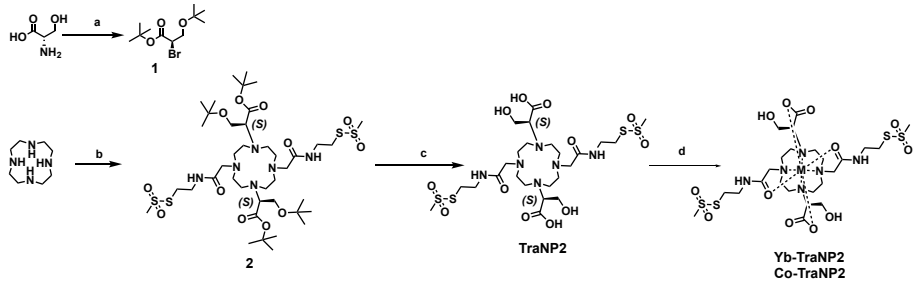


**Scheme 3.1** Synthesis route of TraNP2 a). i) D-Serine, KBr, HBr, $NaNO_2$, $H_2O$, -15 °C, 16 h; ii) *p*-toluenesulfonic acid monohydrate, 2-methylprop-1-ene, rt, 72 h; b) i) compound 1, DIPEA, ACN, rt, 48 h; ii) S-(2-(2-bromoacetamido)ethyl) methanesulfonothioate, $K_2CO_3$, ACN, rt, 48 h; c) TFA: DCM (2:3, *v*:*v*), rt, 10 h; d) ACN, rt, 3 h.

methanesulfonothioate in the presence of $K_2CO_3$ to give **2** in 55% yield after purification. For the deprotection of all the *t*Bu groups, a mixture of TFA:DCM (2:3, *v*:*v*) was used and the crude product was purified by HPLC with 0.2% TFA and a 15-20% acetonitrile gradient on C18 preparative column, yielding 63% of TraNP2.

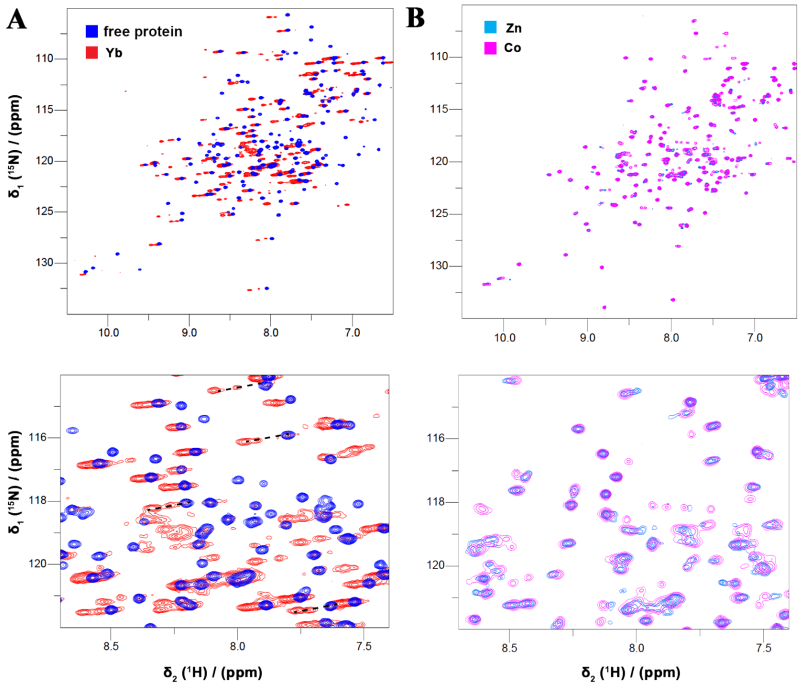


**Figure 3.2** Overlay of $^{1}H$-$^{15}N$ HSQC spectra of T4Lys K147C/T151C (blue) linked to Yb(III) (red) loaded TraNP2 ((**A**), full spectrum (top), zoom in spectrum (bottom)), or Co(II) (magenta) and Zn(II) (sky blue) loaded TraNP2 (**B**), full spectrum (top), zoom in spectrum (bottom)). The NMR spectra were recorded at 14.1 T (600 MHz).

**Protein labeling and NMR spectroscopy.** The uniformly $^{15}N$ enriched T4Lys K147C/T151C were treated with DTT to reduce possible intermolecular disulfide bonds, the DTT was removed and the proteins were incubated with Co(II)/Zn(II)/Yb(III)-TraNP2. The tagged proteins were purified using size exclusion chromatography and the tagging efficiency was determined by MS and NMR. Mass spectrometry results of Co(II)-TraNP2 T4Lys (19333 ± 2 Da) and Yb(III)-TraNP2 T4Lys (19445 ± 2 Da) agreed with the theoretical values of 19334 Da and 19446 Da, respectively, for 98% enrichment of $^{15}N$, suggesting that the probes were attached via two arms and the metal ion was tightly bound and more than 95% of the protein was labeled (App. Figure A3.1). The labeled proteins were used for NMR measurements at a concentration of 100-200 μM. Figure 3.2 shows the overlay HSQC spectra of two pairs samples. For Yb(III)-TraNP2 labeled and free T4Lys, two sets of PCS were detected for most cross peaks in the spectra (Figure 3.2 A). This indicates that at least two conformers of Yb(III)-TraNP2 were present with a different Δχ-

tensor, causing double resonances for an amide spin. Similar results were reported for a published probe-CLaNP3 (Caged Lanthanoid NMR Probe # 3, Figure 3.1).[26] Thus, two chiral branched side-arms cannot effectively reduce the number of conformers of DOTA based complexes. In the spectra of T4Lys tagged with Co(II)/Zn(II)-TraNP2 (Figure 3.2 B), small PCS were observed.

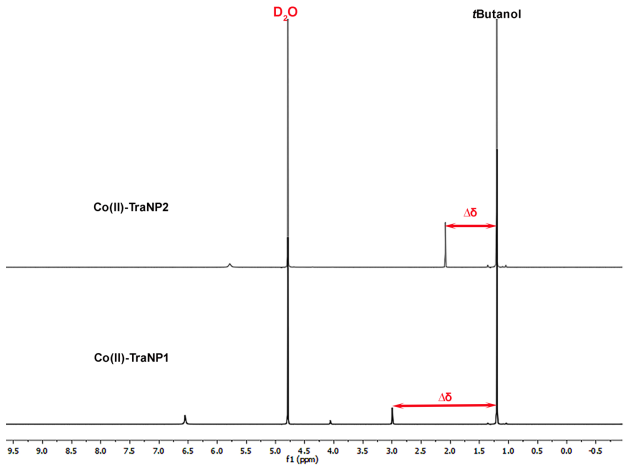


**Figure 3.3** $^{1}$H NMR spectra of Co(II)- TraNP2 and Co(II)-TraNP1 measured by Evans' method. The NMR spectra were recorded at 9.4 T (400 MHz) and 293K.

**Evans' method**. It is surprising that the Co(II) sample showed so few paramagnetic effects. We tested how paramagnetic the sample actually was. In 1953, D. F. Evans proposed a method to determine magnetic susceptibility of paramagnetic molecules in solution using a NMR approach.[27] It is based on bulk magnetic susceptibility shifts (BMS)[28,29] of an inert compound caused by the presence of the paramagnetic molecule. This method has frequently been applied in coordination chemistry to detect the spin-states and effective magnetic moments.[30–33] Here, we use this method to investigate the paramagnetic properties of Co(II)-TraNP1 and Co(II)-TraNP2. Both of the complexes generated BMS for the inert compound tertiary butanol, 720 Hz for TraNP1 and 352 Hz for TraNP2, respectively, indicating the Co(II) ions in both complexes are paramagnetic (Figure 3.3). Using equation 3.1 to 3.3 (Materials and Methods), the effective magnetic moment in Bohr magnetons ($\mu_{B,\,eff}$) of TraNP2 is 5.05. For TraNP1, it is 3.31.

It is remarkable that the Co(II)-TraNP2 probe does not cause significant PCS, despite having a large magnetic moment. The results suggest that the coordination is such that the magnetic susceptibility is isotropic, effectively cancelling the pseudocontact effect. Note that Evans' method measure the total magnetic susceptibility $\chi$, whereas the

PCS is a result of the anisotropy of $\chi$. As was reported in chapter II, the size of the anisotropy varies widely for different Co(II) complexes and can even be different between enantiomers and for one and the same probe tagged to different proteins.

In conclusion, modification of DOTA coordination arms with chiral carbons with methylene hydroxy groups as substituents can modulate the coordination properties to make them suitable for binding to both Ln(III) and 3d-block ions. Unfortunately, TraNP2 is not suitable as a probe for protein NMR because the Yb(III) complex yields double resonances, whereas the Co(II) complex displays an isotropic magnetic susceptibility.

**Materials and Methods**

**General**: cyclen, 2-(aminoethyl)methanethiosulfonate hydrobromide, methyl (S)-oxirane-2-carboxylate, N-(tert-Butoxycarbonyloxy)succinimide, $Ln(OAc)_3$, $CoCl_2{\cdot}6H_2O$, $ZnI_2$, $MnCl_2{\cdot}4H_2O$, methyl (R)-oxirane-2-carboxylate and all other chemicals were purchased and used without further purification. Solvents were purchased from Honeywell, BIOSOLVE or Aldrich and directly use for synthesis. Superdex 75 columns and Sephadex G-25 PD10 desalting columns were purchased from GE Healthcare. Reactions were followed by TLC analysis on silica gel (F 1500 LS 254 Schleicher and Schuell, Dassel, Germany); visualized by UV and/or ninhydrin, $KMNO_4$. Flash chromatography was performed with Screening Devices silica gel 60 (0.04-0.063 mm). A Waters preparative HPLC system, equipped with a Waters C18-Xbridge 5 µm OBD (30 x 150 mm) column and Äkta Basic FPLC (GE Healthcare Inc.) system were used for purification. NMR spectra were recorded on a Bruker AV-400 (400/100 MHz), AV-500 (500/125 MHz) or AV-600 (600/150 MHz) spectrometer. A LCQ liquid chromatography mass spectrometry system and a Finnigan LTQ Orbitrap system were used for high-resolution mass spectrometry and protein conjugation analysis. Thermo Finnigan LCQ Advantage MAX used for liquid chromatography (LC)-mass spectrometry (MS) analysis. Thermo Scientific™ NanoDrop 2000 spectrophotometers were used for protein concentration measurement.

**Protein labeling:** To link M-TraNP2 to $^{15}N$ labelled T4Lys produced as described in chapter II. The yield of labeling estimated from the LC-MS and NMR, was more than 95%.

**Protein NMR spectroscopy:** The NMR samples of T4lys-Metal-TraNP2 (100–200 µM) were prepared in 30 mM sodium phosphate pH 5.5 buffer containg 100 mM NaCl, and 6% (*v/v*) $D_2O$. All $^1H$-$^{15}N$ HSQC were recorded on a Bruker AV-600 (600 MHz) spectrometer, at 298 K. Data were processed with Topspin 3.5 and analyzed with CcpNmr Analysis version 2.4.0. T4Lys resonances assignments were provided by Dr. Simon P. Skinner based on previous work.

**Evans' method:** A pair of coaxial NMR tubes with different diameter was required for this method. A melting point capillary was used as inter tube and a 5 mm NMR tube was used as an outer tube. Co(II)-TraNP2 (2.5 mg, 3.15 µmol) was dissolved in $D_2O$ (157 µL,

containing 2% (*v/v*) tertiary butanol). This solution (100 μL) was carefully transferred into a melting point capillary (inter tube) before it was zipped. The 5 mm NMR tube contained 500 μL of $D_2O$ with 2% (*v/v*) tertiary butanol. The above zipped melting point capillary was transferred into the 5 mm NMR tube at the bottom. The spectra were acquired at 9.4 T (400 MHz) on a Bruker NMR spectrometer. For Co(II)-TraNP1 the sample contained 13.5 μmol in 116 μL $D_2O$ with 2% (*v/v*) tertiary butanol. By measuring the chemical shifts difference of an inert compound, the tertiary butanol, in the presence and absence of a paramagnetic compound, the effective magnetic moment in Bohr magnetons ($\mu_{eff}$) of the paramagnetic compound can be calculated with equation 3.1 to 3.3.[27,31,32,34]

$$\mu_{eff} = 2.84\sqrt{\chi_p T} \quad 3.1$$

$$\chi_p = \frac{3\times10^3\Delta f}{4\pi f_m C} - \chi_D \quad 3.2$$

$$\chi_D \approx -\frac{M}{2}\times 10^{-6} \quad 3.3$$

$\chi_P$ (in emu/mol) is the corrected paramagnetic molar susceptibility defined by equation 3.2; T (in K) is the absolute temperature for the measurement. $\Delta f$ (in Hz) is the chemical shift difference of the inert compound in the presence and absence of the paramagnetic compound; $f_m$ (in Hz) is external magnetic field, C (in mole/L) is the concentration of the paramagnetic compound; $\chi_D$ (in emu/mol) is the diamagnetic susceptibility and M (in g/mol) is the molecular mass.

**Synthesis**

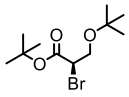

**Tert-butyl (*R*)-2-bromo-3-(tert-butoxy) propanoate, compound 1**

To a three necked flask equipped with a magnetic stirring bar and gas inlet tube, KBr (11.4 g, 96.9 mmol) and D-Serine (3 g, 28.5 mmol) were dissolved in $H_2O$ (50 mL), and cooled to -15 °C. A wash bottle containing 1 M KOH solution connected to the flask and $N_2$ gas pass through it. Then HBr solution (48%, 7 mL) was added to the reaction mixture, followed by six portions of $NaNO_2$ (2.4 g, 34.8 mmol) added (~0.4 g every 20 mins). The reaction mixture was allowed to warm to 0 °C and stirring was continued for 16 h. The reaction mixture was flushed with $N_2$ and extracted with diethyl ether (3 x 20 mL), dried ($Na_2SO_4$) and concentrated under reduced pressure. Without further purification, 1 g (~6.57 mmol) of the crude compound was dissolved in DCM (50 mL) in a DURAN bottle and at 0 °C treated with *p*-toluenesulfonic acid monohydrate (1.25 g, 6.57 mmol) and with 2-methylprop-1-ene (10 mL). After 72 h at rt, the reaction mixture was washed with sat. $NaHCO_3$ solution (25 mL) and water (25 mL), dried ($Na_2SO_4$) and concentrated. The residue was purified with silica flash column chromatography (10% of diethyl ether in pentane) to give 1.62 g (88 %) compound **1** as a slightly yellow oil. The spectroscopic data were in agreement with those reported in the literature: $^1$H NMR (400 MHz, $CDCl_3$, 293K): **δ** = 1.16 (s, 9H), 1.46 (s, 9H), 3.57-3.60 (d, 1H), 3.75-3.79 (t, 1H), 4.05-4.09 (d, 1H). $^{13}$C NMR (400 MHz, $CDCl_3$, 293K): **δ** = 27.41 ($CH_3C$), 27.74 ($CH_3C$), 63.69

($CH_2OtBu$) 74.00 ($C(CH_3)_3$), 82.23 ($C(CH_3)_3$), 167.83 (COOtBu). $[\alpha]_D^{20}$= -3.1 (C= 10 mg/mL, Methanol). FTIR ($cm^{-1}$): 2982.1, 2923.4, 2844.7, 1054.6, 1033.1, 1010.3.

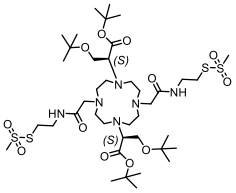

**Di-tert-butyl2,2'-(4,10-bis(2-((2-((methylsulfonyl)thio)ethyl)amino)-2-oxoethyl)-1,4,7,10-tetraazacyclododecane-1,7-diyl)(2S,2'S)-bis(3-(tert-butoxy)propanoate), compound 2**

Cyclen (0.5 g, 2.9 mmol) in acetonitrile (30 mL) was mixed with compound **1** (1.65 g, 5.8 mmol) and DIPEA (1.5 mL, 8.7 mmol) and stirring was continued at rt for 48 h. Without purification, the resulting mixture was mixed with S-(2-(2-bromoacetamido)ethyl) methanesulfonothioate (3.22 g, 11.6 mmol) and $K_2CO_3$ (1.6 g, 11.6 mmol). After stirring at rt for 48 h, $K_2CO_3$ was removed by filtration, the mixture concentrated and the residue purified by silica gel flash column chromatography (7% of MeOH in DCM) to give the title compound as a white solid, 0.79 g (31% yield). $^1$H NMR (500 MHz, MeOD, 298K): **δ** = 1.20-1.21 (d, 18H), 1.52-1.54 (d, 18H), 1.99-2.09 (m, 4H), 2.26-2.34 (d, 2H), 2.48-2.56 (d, 2H), 2.62-2.77 (m, 4H), 3.34-3.39 (m, 2H), 3.41-3.42 (q, 6H), 3.50-3.57 (m, 3H), 3.60-3.72 (m, 4.5H), 3.75-3.89 (m, 5.5 H), 3.34-3.39 (m, 2H). $^{13}$C NMR (500 MHz, MeOD, 298 K): **δ** = 27.76, 28.56, 37.07, 39.78, 47.06, 50.93, 57.49, 82.55, 200.77. HR-MS: m/z 963.4626 $[M+H]^+$, calcd. $[C_{40}H_{78}N_6O_{12}S_4]$ 963.4639. $[\alpha]_D^{20}$= 8.1 (C= 1 mg/mL, methanol). FTIR ($cm^{-1}$): 1682.8, 1204.9, 1186.3, 1136.2, 1033.1, 844.3, 802.8, 724.1.

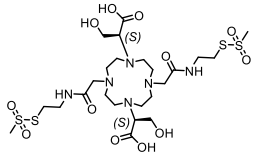

**(2S,2'S)-2,2'-(4,10-bis(2-((2-((methylsulfonyl)thio)ethyl)amino)-2-oxoethyl)-1,4,7,10-tetraazacyclododecane-1,7-diyl)bis(3-hydroxypropanoic acid), TraNP2**

Compound **2** (0.1 g, 0.11 mmol) was dissolved in TFA:DCM (2:3, *v:v*) while stirring at rt for 10 h. The reaction mixture was concentrated and the residue purified by reverse phase HPLC (0.2% TFA and a 10-15% acetonitrile gradient on C18 preparative column), yielding 0.05 g (63% yield) TraNP2. $^1$H NMR (500 MHz, MeOD, 343 K): **δ** = 3.22 (br, 6H), 3.38 (m, 4H), 3.36-3.43 (br, 2H), 3.54-3.64 (m, 8H), 3.43 (s, 6H), 3.41-3.56 (br, 8H), 3.69-3.87 (dd, 4H), 4.12-4.16 (m, 4H). $^{13}$C NMR (500 MHz, MeOD, 343 K): **δ** = 36.45 ($CH_2SO_2$), 40.29 ($CH_2CH_2SO_2$) 51.83 ($CH_2N$), 50.96 ($CH_3S$), 56.19 ($CH_2CONH$), 60.05 ($CH_2OH$), 64.63 ($CHCH_2OH$). $[\alpha]_D^{20}$= 8.0 (C= 2 mg/mL, methanol). HR-MS: m/z 739.2145 $[M+H]^+$, calcd. $[C_{24}H_{46}N_6O_{12}S_4]$ 739.2050. FTIR (ν $cm^{-1}$): 1684.2, 1203.4, 1130.5, 1054.6, 1033.1, 1013.11, 835.7, 801.3, 748.3, 721.2.

**Metal complexes**: To a solution of TraNP2 (20.7 mg, 28 µmol) in 280 µL ACN, 1.1 equiv. $CoCl_2{\cdot}6H_2O$ or $ZnI_2{\cdot}6H_2O$ or $Yb(CH_3COO)_3{\cdot}4H_2O$ was added. The mixture stirred at rt for 3 h and the formation of metal complex was checked by LC/MS. Without further purification, Co-TraNP2 was used to protein sample labeling. The other metal ions $Zn^{2+}$

and $Yb^{3+}$ were chelated to TraNP2 following the same procedure. Co-TraNP2 HR-MS: m/z 796.1319 $[M+H]^+$, calcd. $[C_{24}H_{44}CoN_6O_{12}S_4]$ 796.1232; Zn-TraNP2 HR-MS: m/z 401.0667 $[M+2H]^{2+}$, calcd. $[C_{24}H_{44}ZnN_6O_{12}S_4]$ 401.0596; Yb-TraNP2-SS HR-MS: m/z 913.1520 $[M+H]^+$, calcd. $[C_{24}H_{44}YbN_6O_{12}S_4]$ 913.1523.

**References**


(1) Nitsche, C.; Otting, G. Pseudocontact Shifts in Biomolecular NMR Using Paramagnetic Metal Tags. *Prog. Nucl. Magn. Reson. Spectrosc.* **2017**, *98–99*, 20–49.

(2) Su, X. C.; Otting, G. Paramagnetic Labelling of Proteins and Oligonucleotides for NMR. *J. Biomol. NMR* **2010**, *46* (1), 101–112.

(3) Keizers, P. H. J.; Ubbink, M. Paramagnetic Tagging for Protein Structure and Dynamics Analysis. *Prog. Nucl. Magn. Reson. Spectrosc.* **2011**, *58* (1–2), 88–96.

(4) Liu, W. M.; Overhand, M.; Ubbink, M. The Application of Paramagnetic Lanthanoid Ions in NMR Spectroscopy on Proteins. *Coord. Chem. Rev.* **2014**, *273–274*, 2–12.

(5) Otting, G. Prospects for Lanthanides in Structural Biology by NMR. *J. Biomol. NMR* **2008**, *42* (1), 1–9.

(6) Nguyen, T. H. D.; Ozawa, K.; Stanton-Cook, M.; Barrow, R.; Huber, T.; Otting, G. Generation of Pseudocontact Shifts in Protein NMR Spectra with a Genetically Encoded Cobalt(II)-Binding Amino Acid. *Angew. Chemie. Int. Ed.* **2011**, *123*, 718–720.

(7) Yang, Y.; Huang, F.; Huber, T. Site-Specific Tagging Proteins with a Rigid , Small and Stable Transition Metal Chelator, 8-Hydroxyquinoline, for Paramagnetic NMR Analysis. *J. Biomol. NMR* **2016**, *64* (2), 103–113.

(8) Bahramzadeh, A.; Jiang, H.; Huber, T.; Otting, G. Two Histidines in an **α**-Helix: A Rigid $Co^{2+}$-Binding Motif for PCS Measurements by NMR Spectroscopy. *Angew. Chemie. Int. Ed.* **2018**, *57* (21), 6226–6229.

(9) Dvoretsky, A.; Gaponenko, V.; Rosevear, P. R. Derivation of Structural Restraints Using a Thiol-Reactive Chelator. *FEBS Lett.* **2002**, *528* (1–3), 189–192.

(10) Moshref, A.; Otting, G.; Sharipo, A.; Pintacuda, G.; Leonchiks, A. Site-Specific Labelling with a Metal Chelator for Protein-Structure Refinement. *J. Biomol. NMR* **2004**, *29* (3), 351–361.

(11) Park, S. H.; Wang, V. S.; Radoicic, J.; De Angelis, A. A.; Berkamp, S.; Opella, S. J. Paramagnetic Relaxation Enhancement of Membrane Proteins by Incorporation of the Metal-Chelating Unnatural Amino Acid 2-Amino-3-(8-Hydroxyquinolin-3-yl)Propanoic Acid (HQA). *J. Biomol. NMR* **2015**, *61* (3–4), 185–196.

(12) Kauffman, G. B. Theories of Coordination Compounds. *J. Chem. Educ.* **1986**, 63(4), A116.

(13) Venkataraman, D.; Du, Y.; Wilson, S. R.; Hirsch, K. A.; Zhang, P.; Moore, J. S. A Coordination Geometry Table of the d-Block Elements and Their Ions. *J. Chem. Educ.* **1997**, *74* (8), 915–918.

(14) Van Vleck, J. H. Theory of the Variations in Paramagnetic Anisotropy among Different Salts of the Iron Group. *Phys. Rev.* **1932**, *41* (2), 208–215.

(15) Newman, D. J; Ng, B. K. C. *Crystal Field Handbook*; Cambridge University Press: Cambridge, 2000.

(16) Nielsen, L. G.; Junker, A. K. R.; Sørensen, T. J. Composed in the F-Block: Solution Structure and Function of Kinetically Inert Lanthanide(III) Complexes. *Dalt. Trans.* **2018**, *47* (31), 10360–10376.

(17) Chau, O.; Goeleven, D.; Oujja, R. Variational Inequality Models Arising in the Study of

Viscoelastic Materials. *Coord. Chem. Rev.* **2000**, *196*, 165–195.

(18) Man, B.; Su, X. C.; Liang, H.; Simonsen, S.; Huber, T.; Messerle, B. A.; Otting, G. 3-Mercapto-2, 6-Pyridinedicarboxylic Acid: A Small Lanthanide-Binding Tag for Protein Studies by NMR Spectroscopy. *Chem. Eur. J.* **2010**, *16* (12), 3827–3832.

(19) Keizers, P. H. J.; Saragliadis, A.; Hiruma, Y.; Overhand, M.; Ubbink, M. Design, Synthesis, and Evaluation of a Lanthanide Chelating Protein Probe: CLaNP-5 Yields Predictable Paramagnetic Effects Independent of Environment. *J. Am. Chem. Soc.* **2008**, *130* (44), 14802–14812.

(20) Liu, W.-M.; Keizers, P. H. J.; Hass, M. A. S.; Blok, A.; Timmer, M.; Sarris, A. J. C.; Overhand, M.; Ubbink, M. A pH-Sensitive, Colorful, Lanthanide-Chelating Paramagnetic NMR Probe. *J. Am. Chem. Soc.* **2012**, *134* (41), 17306–17313.

(21) Brittain, H. G.; Desreux, J. F. Luminescence and NMR Studies of the Conformational Isomers of Lanthanide Complexes with an Optically Active Polyaza Polycarboxylic Macrocycle. *Inorg. Chem.* **1984**, *23* (26), 4459–4466.

(22) Suchý, M.; Li, A. X.; Milne, M.; Bartha, R.; Hudson, R. H. E. DOTMA-Based Amides (DOTMAMs) as a Platform for the Development of PARACEST MRI Contrast Agents. *RSC Adv.* **2016**, *6* (67), 62647–62655.

(23) Meyer, M.; Dahaoui-Gindrey, V.; Lecomte, C.; Guilard, R. Conformations and Coordination Schemes of Carboxylate and Carbamoyl Derivatives of the Tetraazamacrocycles Cyclen and Cyclam, and the Relation to Their Protonation States. *Coord. Chem. Rev.* **1998**, *178–180*, 1313–1405.

(24) Gilsoul, D.; Jacques, V.; Mesbahi, M.; Hermann, M.; Desreux, J. F.; Sauvage, C.; Humblet, V.; Comblin, V. Designing New MRI Contrast Agents: A Coordination Chemistry Challenge. *Coord. Chem. Rev.* **2002**, *185–186*, 451–470.

(25) C. Eichenauer, N.; Tschersich, R.; Pietruszka, J. Total Synthesis of Solandelactone I. *J. Nat. Prod.* **2015**, *78* (11), 2782–2790.

(26) Vlasie, M. D.; Comuzzi, C.; Van Den Nieuwendijk, A. M. C. H.; Prudêncio, M.; Overhand, M.; Ubbink, M. Long-Range-Distance NMR Effects in a Protein Labeled with a Lanthanide-DOTA Chelate. *Chem. Eur. J.* **2007**, *13* (6), 1715–1723.

(27) Evans, D. F. 400. The Determination of the Paramagnetic Susceptibility of Substances in Solution by Nuclear Magnetic Resonance. *J. Chem. Soc.* **1959**, *0*, 2003–2005.

(28) Dickinson, W. C. The Time Average Magnetic Field at the Nucleus in Nuclear Magnetic Resonance Experiments. *Phys. Rev.* **1951**, *81* (5), 717–731.

(29) Chu, K. -. C.; Xu, Y.; Balschi, J. A.; Springer, C. S. Bulk Magnetic Susceptibility Shifts in Nmr Studies of Compartmentalized Samples: Use of Paramagnetic Reagents. *Magn. Reson. Med.* **1990**, *13* (2), 239–262.

(30) Evans, D. F.; James, T. A. Variable-Temperature Magnetic-Susceptibility Measurements of Spin Equilibria for Iron(III) Dithiocarbamates in Solution. *J. Chem. Soc. Dalt. Trans.* **1979**, 4, 723–726.

(31) Loliger, J.; Scheffold, R. Paramagnetic Moment Measurements by NMR A Micro Technique. *J. Chem. Educ.* **2009**, *49* (9), 646.

(32) De Buysser, K.; Herman, G. G.; Bruneel, E.; Hoste, S.; Van Driessche, I. Determination of the Number of Unpaired Electrons in Metal-Complexes. A Comparison between the Evans' Method and Susceptometer Results. *Chem. Phys.* **2005**, *315* (3), 286–292.

(33) Nataro, C.; Fosbenner, S. M. Synthesis and Characterization of Transition-Metal Complexes Containing 1,1′-Bis(Diphenylphosphino)Ferrocene. *J. Chem. Educ.* **2009**, *86* (12), 1412.

(34) Schubert, E. M. Utilizing the Evans Method with a Superconducting NMR Spectrometer in

the Undergraduate Laboratory. *J. Chem. Educ.* **1992**, *69* (1), 62.